International Journal of Signal Processing, Image Processing and Pattern Recognition
Vol.8, No.10 (2015), pp.257-270
http://dx.doi.org/10.14257/ijsip.2015.8.10.27

Study on Urban Remote Sensing Classification Based on Improved RBF Network and Normalized Difference Indexes

Xiaobo Luo [1,2], Wenya Zhao[3], Shiqiang Wei [1] and Qinghua Fu[4]

[1] *Institute of Resources and Environment, Southwest China University, Chongqing 400715, China;*
[2] *Institute of Computer Science and Technology, Chongqing University of Post and Telecommunications, Chongqing 400065, China;*
[3] *Chongqing Aerospace Vocational and Technological College, 400021, China;*
4 Pearl River Hydraulic Research Institute，Pearl River Water Resources Commission, Guangzhou, Guangdong 510611.
Correspondence should be addressed to sqwei@swu.edu.cn and luoxb@cqupt.edu.cn

Abstract

Aiming at the complexity of ground objects in urban area, and the difficulty in distinguishing ground objects using spectral characteristics, we extracted normalized different indexes, namely Modified Normalized Difference Water Index (MNDWI), Soil Adjusted Vegetation Index (SAVI) and Normalized Difference Building Index (NDBI) , as the key auxiliary information for land use classification of urban area. To solve problems of RBF neural network, such as local minimum values and discrete output value in output layer, we used max-min distance means to initialize RBF center, and introduced equilibrium factor into Gauss function to improve RBF neural network learning algorithm. On this basis, a new urban area classification model was proposed based on improved RBF network and normalized difference indexes. At last, NanChong city in SiChuan province of China was taken as the study area, and TM images was used as experiment data to test the model proposed in this paper. The results showed that, based on the improved RBF network, with the help of spectral band information, the classification overall accuracy was 89.97%, Kappa coefficient was 0.88; using both spectral band information and normalized difference indexes, the classification overall accuracy was 95.02%, Kappa coefficient is 0.94, the classification overall accuracy was improved by 5.05%. Also, the experiment results showed that, with the help of spectral band information and normalized difference indexes, the classification overall accuracy of MLC, BP and improved RBF network was 90.12%, 93.63%, 95.02%, respectively, which means RBF has an advantage of fusing geological parameters in classification.

Keywords: *RBF Network, Normalized Difference Index, Urban Land Use, Classification*

1. Introduction

With the development of remote sensing technology, remote sensing image classification, as an important link in the application of remote sensing technology, is playing an increasingly important role in special information extraction, dynamic change monitoring, thematic mapping, remote sensing image database construction and other fields. There are many advanced classification algorithms which are widely used in remote sensing classification, including neural network, support vector machine [1-4], expert system [5-6], and so on. Among them, the neural network algorithms can work well

ISSN: 2005-4254 IJSIP

without prior knowledge of data distribution, has the good characteristics of error tolerance and strong adaptability, and can easily integrate different types of data [7-11].

Radial basis function (RBF) neural network has been studied and applied widely in remote sensing image classification, which is a kind of forward neural network combined with a parameterized statistical distribution model and a Non parametric linear perception model [12-17]. Compared with the BP neural network, the RBF neural network has advantages of fast learning speed, not easy falling into local minima, and so on [12,15]. The precision and stability of the RBF neural network algorithm depends on the reasonable selection of the center and width of the hidden layer. At present, the design methods of the center of the hidden layer includes k-means algorithm, competitive learning algorithm, self-organizing neural network clustering algorithm, and so on. However, the above clustering algorithms can easily be trapped into local minima because of the random initialization of the RBF centers. It is difficult to get the optimal design of the hidden layer, and the classification effect of classifier is affected [15-18]. At the same time, the value of output layer is very discrete because Gauss kernel function is used in the RBF neural network [20].

On the other hand, the main input features are the original spectral features and texture features [20-22], shape features [23-24], and so on. The indexes with physical significance from the original spectral information are rarely used, which limits the classification accuracy in complex urban area.

As for the urban area, the ground objects are complex, the spatial distribution is discrete, and the phenomenon of same object with different spectra and different objects with same spectrum is serious. This paper mainly aims at the above problems of remote sensing classification in city area. The maximum minimum distance method is used to initialize RBF center, and the equilibrium factor is introduced in Gauss function, to improve RBF neural network learning algorithm. Further, combined with the normalized spectral indexes and RBF neural network, the remote sensing classification model is established to improve the classification accuracy of city area.

2. Research Methods

2.1. Data Preprocessing and Normalized Difference Indexes Extraction

The experiment data source are TM 5 images obtained on May 23, 2010. Image bands 1-5 and 7 are visible band and near-infrared band, of which their spatial resolutions are 30 m; Band 6 is the thermal infrared band, of which spatial resolutions is 120 m. Also, in this research, auxiliary data like land use map and QuickBird image were referenced. Data preprocessing was mainly completed in ENVI 4.3. Firstly, the raw images was geo-referenced based on the QuickBird images, and was re-sampled with a pixel size of 30 m by 30m for all bands. The RMSE of rectification was less than 1.0 pixel. Next, after radiometric calibration and atmospheric correction by the FLAASH tool, the surface reflections of six optical bands were obtained.

According to pixel scale, the urban surface is mainly composed of three kinds of objects: vegetation, construction land and water. Vegetation is mainly composed of grassland, cultivated land, roads and bare land. Water is composed of lakes and rivers. In this paper, NDVI, NDBI and MNDWI having physical guiding significance were used to represent the coverage of vegetation, construction land and water, respectively.

NDVI means normalized difference vegetation index, it can show the vegetation coverage condition relatively well. It is also one of the most widely used index. Because NDVI is often interfered by the soil background noise, Huete put forward a Soil Adjusted Vegetation Index (SAVI). SAVI can be obtained by the formula below [26]:

$$SAVI = \frac{(\rho_{NIR} - \rho_R)}{\rho_{NIR} + \rho_R + L}(1+L) \quad (1)$$

In this formula, L is the soil adjusted factor, its value is between 0 to 1. Usually, setting it 0.5 could weaken soil background difference, further eliminate noise fairly well. Because of the introduction of soil adjusted factor, SAVI is considered suitable for the low vegetation coverage region, such as urban area.

Normalized Difference Building Index (NDBI) is proposed by Cha Yong based on imitating normalized difference vegetation index, which can more accurately reflect the construction land information, the greater NDBI is, the greater the proportion of construction land is, and the higher building density is in that area. Its expression is as follow[27]:

$$NDBI = \frac{\rho_{MIR} - \rho_{NIR}}{\rho_{MIR} + \rho_{NIR}} \quad (2)$$

McFeeters (1996) constructed Normalized Difference Water Index (NDWI) using the reflection difference of water between green band and near-infrared band [28]. Xu HanQiu(2005) put forward the Modified Normalized Difference Water Index (MNDWI) using short wave infrared band instead of near infrared band in, which can enhance the contrast between water and other ground, also restrain inhibit the noise of buildings and soil background. And its formula is as follow [29]:

$$MNDWI = \frac{\rho_G - \rho_{MIR}}{\rho_G - \rho_{MIR}} \quad (3)$$

In the above formula (1) ~ (3), ρ_G、 ρ_R、 ρ_{NIR}、 ρ_{MIR} represent the surface reflection of green band, infrared band, near-infrared band and middle infrared band, respectively. As for TM image, they indicate the surface reflection of TM band 2, 3, 4 and 5, respectively.

2.2. Improved Learning Algorithm of RBF Neural Network

RBF neural network is a nonlinear mapping neural network model that combines unsupervised clustering method with supervised monolayer linear perception essentially. RBF is composed of three layers, namely input layer, middle RBF layer, output layer. Usually the number of nodes of input layer equals the number of dimensions of data used in application field, and the number of nodes in output layer is equal to the number of classes.

Three steps are included in RBF neural network learning algorithm [12-17]: First, to determine the centers of RBF by unsupervised method; Secondly, to calculate the width of RBF centers; Thirdly, to determine the connection weight between middle layer and output layer. However, there are some defects in RBF neural network learning algorithm: usually the center is initialized randomly in the process of determining RBF centers by unsupervised method. So the clustering algorithms can easily be trapped into local minima, and it is difficult to get the optimal hidden layer. The output values could be very discrete as Gaussian kernel function is used, even for the same class. Aiming at these problems, combined with the practical application in urban remote sensing classification, an improved RBF neural network learning algorithm was put forward as follows:

(1) Input the unsupervised sample set $X = \{x_i, \quad i = 0,1,..., P-1\}$, then use max-min distance Means to initialize the hidden layer center $c_j(0)$, and use competitive learning algorithm to train the hidden layer center iteratively [30-31]. Below are details:

$$
\begin{aligned}
&c_{jm}(0) = MaxMinDist\{X\}, m = 0,1,..., I-1,\ j = 0,1,..., N-1, t = 0 \\
&whil\ \ ((\Delta c_j \geq \varepsilon_1)\ \ or\ \ (t \leq T_1)) \\
&\{ \\
&\quad j^* = \arg\ \ [\min(\| x - c_j(t) \|)],\ j = 0,1,..., Q-1 \\
&\quad c_j(t+1) = c_j(t) + \frac{a_0}{(1+t/T_1)} * [x - c_j(t)], \quad j = j^* \\
&\quad \Delta c_j = \| c_j(t+1) - c_j(t) \|, t = t+1 \\
&\}
\end{aligned}
\tag{4}
$$

In the above formula , j^* represents the number of winning node, $\arg[\min(*)]$ represents number of min distance node obtained, $\| * \|$ represents Euclidean distance, t represents the times of iterations, T_1 is the final times of iterations, a_0 is the initial learning rate, Δc_j and ε_1 are the change of RBF center and error threshold in two successive iterations.

(2) Calculate the width of RBF σ_j

$$
\sigma_j{}^2 = \frac{1}{M} \sum_{x \in \theta_j} (x - c_j)^T (x - c_j) \tag{5}
$$

In above formula, θ_j represents the jth class, M represents the number of samples that belong to θ_j

(3) Load training sample set X and class information, use gradient descent algorithm to train the connection weight between RBF layer and output layer [15-17]. The expressions are shown as follows:

$$
\begin{aligned}
&W_{kj}(0) = random(0,\ \ 0.1),\ j = 0,1,..., N-1, k = 0,1,..., M-1, t = 0 \\
&while\ \ ((\Delta W_k \geq \varepsilon_2)\ \ or\ \ (t \leq T_2)) \\
&\{ \\
&\quad O_j = \exp(-\frac{\| x - c_j \|^2}{2K\sigma_j{}^2}) \\
&\quad O_k = \sum_{j=0}^{N-1} W_{jk} O_j \\
&\quad W_{kj}(t+1) = W_{kj}(t) + \frac{\eta_0}{(1+t/T_2)} * (O_k - T_k) * O_j \\
&\quad \Delta W_k = \| W_k(t+1) - W_k(t) \|, t = t+1 \\
&\}
\end{aligned}
\tag{6}
$$

In above expression, O_j is the output valve of hidden layer node j; O_k is the real output valve of output node k, T_k is the ideal output valve of output node, W_{kj} is the connection weight between output layer node k and hidden layer node j; η_0 is the initial learning rate, K is the equilibrium factor, t is the times of iterations , T_2 is total times of iterations, η_0 is the initial learning rate in the process of RBF clustering,

ΔW_{jk} is the change of RBF center in two successive iterations. ε_2 is the error threshold.

In this paper, the improvements of RBF neural network learning algorithm are embodied in two respects:

(1) Max-min distance Means was introduced into RBF neural network clustering learning to initialize RBF centers. It solves the defect brought by random clustering center;

(2)When Gauss function is used, the output values could be very discrete, even for the same class model. To get the output valve to accord with the property of clustering, we introduced equilibrium factor K. And its value should be in range [5, 10]. In this paper, it is set as 10. If K is too little, output values cannot be close enough to each other; Also if K is too large, the output values will be too close to each other, and the performance of the entire network will be declined.

2.3. The Urban Classification Model Based on Improved RBF Network

According to the above RBF neural network learning algorithm, combining the concrete application of remote sensing image classification, the urban remote sensing classification model was proposed as shown in Figure 1.

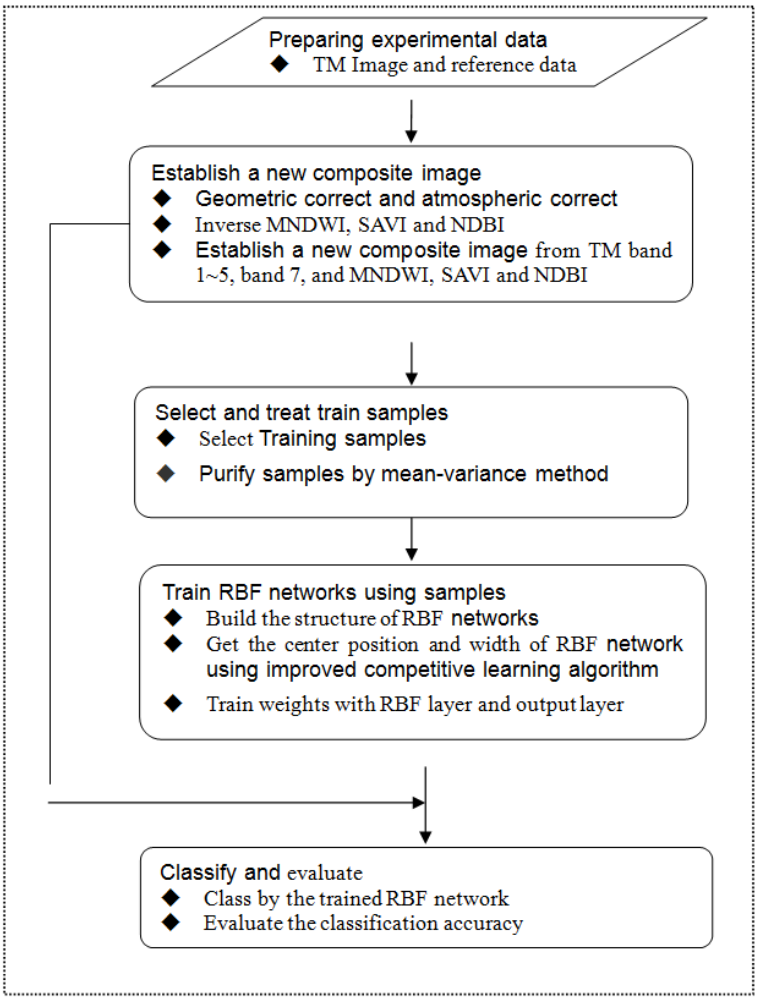

Figure 1. The Urban Remote Sensing Classification Model based on RBF Network

According to Figure 2, several steps are included in the urban remote sensing classification model based on RBF neural network:

(1) SAVI, NDBI and MNDWI were inversed from TM images after atmospheric correction. So there were nine input features together with the surface reflections of the six light bands.

(2) Supervision training samples were chosen, and were preprocessed by mean-variance method.

(3) Supervision training samples were input into the RBF neural network, and were used to train the network: To use max-min distance means to initialize the RBF centers, and use competitive learning algorithm to train RBF centers; To compute the width of RBF according to the samples attributable to the RBF centers; To use gradient descent algorithm to train the connection weight between RBF layer and output layer.

(4) Use the stable RBF neural network to classify those unclassified pixels to the classified image, and evaluate its precision.

3. Experimental Results and Analysis

We chose the area within the ring expressway of Nanchong city, Sichuan province, China, namely the core area of the main city and its rapid expansion surrounding area, as the research area. Its specific location is shown as figure 2. The study area is located in north latitude 30.72~30.86 degree, in east longitude 106.03~106.19 degree, the length along south to north is about 14 kilometers, the width along east to west is about 16 km, and its area is about 233 km^2. The maximum elevation is 489 m, the lowest elevation is 221 m, and the average elevation is 278 m over the study area. The Jialing River goes through the city from north to south direction roughly. This leads to form a slice multi-center and cluster structure because of the natural separation by terrain and rivers.

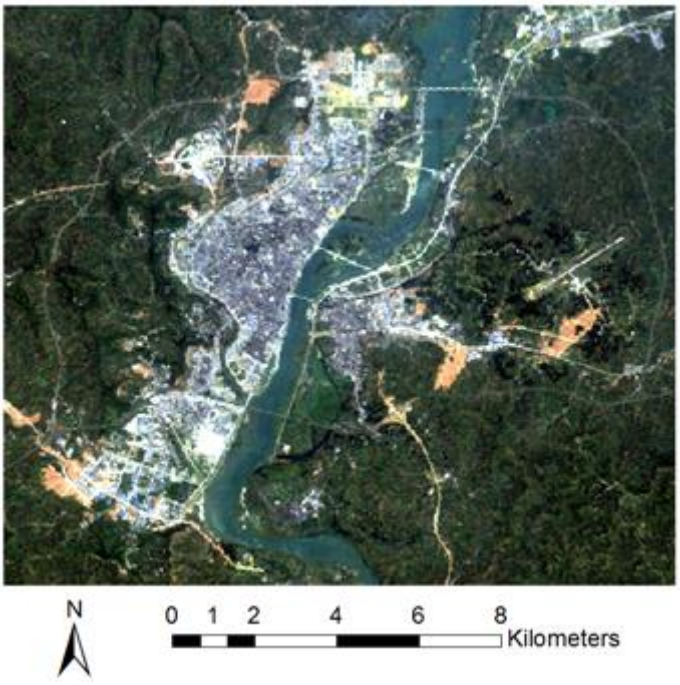

Figure 2. The False-color Image of Study Area (R = TM 3, G = TM 2, B = TM 1)

According to the study area's QuickBird images and other auxiliary data, the ground objects of the study area are identified as 7 categories, which are water, new city, old city, bare land, cultivated land, woodland and vegetable land. Total 5046 training samples were selected from the original image and the samples should be representative and reflective

and can reflect the distribution of the actual surface ground objects. The mean spectral value of the ground objects is shown as figure 3. From figure 3, we can find that the spectral characteristics of old city, new city and bare land are close, especially the spectral features of new city and bare land is very similar, and the spectral distributions of cultivated land, vegetable land and woodland are similar.

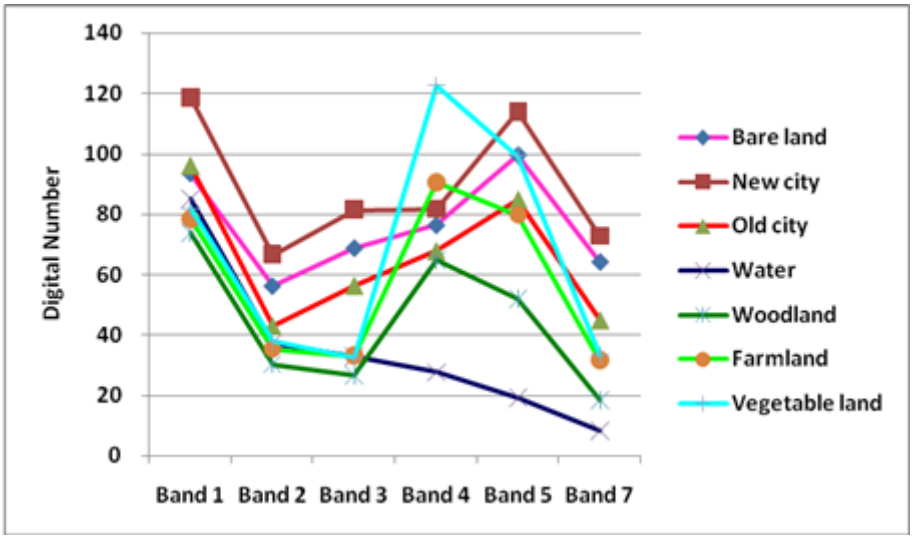

Figure 3. Spectral Distribution Curve of Different Categories

The normalized indexes, namely MNDWI, SAVI and NDBI, were inversed from TM images. The index distribution characteristics of ground objects are shown in figure 4. From figure 4 we can find that three indices are different and can better reflect the changes in urban land use types. Compared to the original spectral values, indexes can better distinguish the land use types of urban areas.

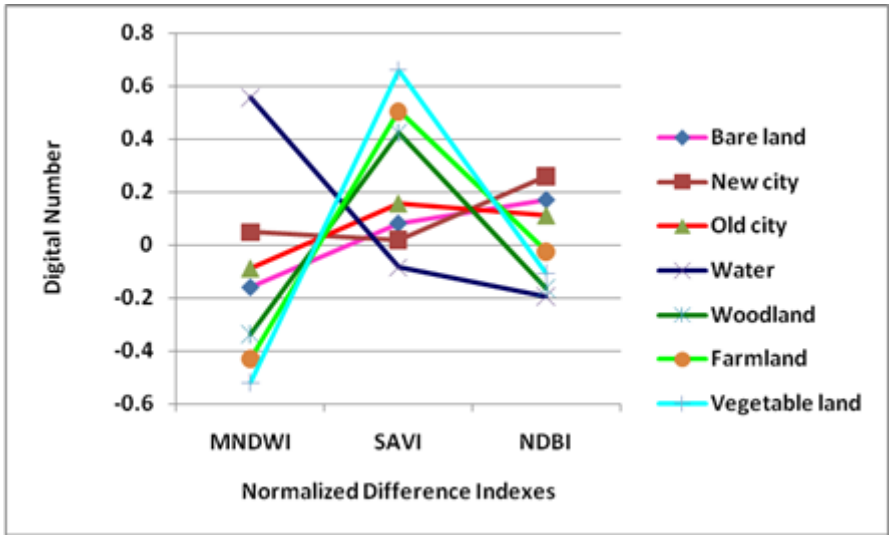

Figure 4. Normalized Difference Index Curve of Different Categories

To analyze and compare the spectral index's effect on classification accuracy, two experiments were carried out. The original spectral information was used in the first experiment, and both the original spectral information and index information were used in the second experiment. In the first experiment, input features include TM band 1-5 and 7,

so the number of input layer nodes is 6. The number of output layer nodes is 7 because the number of the classes of study area is 7.

Because the number of middle RBF nodes is difficult to determine, it is the difficulty of the design of RBF structure. According to several trials, the number of middle RBF nodes was set 20, which can obtain a higher overall classification accuracy. So the network structure was 6-20-7. The Iterations and learning rate of training RBF centers was set to 1200 and 0.2 respectively. The iterations and learning rate of training the weights between RBF layer and output layer was respectively set to 2000 and 0.15 respectively. We used the selected 5046 training samples to train the RBF network, and classified the whole remote sensing image with the trained network. The classification result is shown as figure 5.

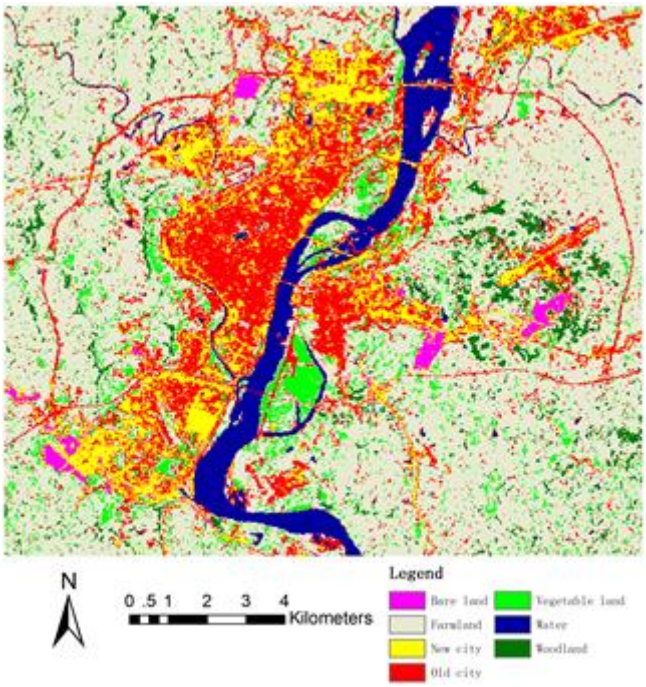

Figure 5. The Classification Using Spectrum Information

When simultaneously using spectral information and index information, the input features include TM band 1~5, 7, SAVI, MNDWI and NDBI. The number of the input layer nodes is 9; and using the same above method, the RBF nodes are set to 25, and the network structure was 9-25-7. The Iterations and learning rate of training RBF centers were set to 2000 and 0.15. The weight iterations and learning rate is respectively set to 3000 and 0.1 when training the weights between RBF layer and output layer. The classification result is shown in figure 6.

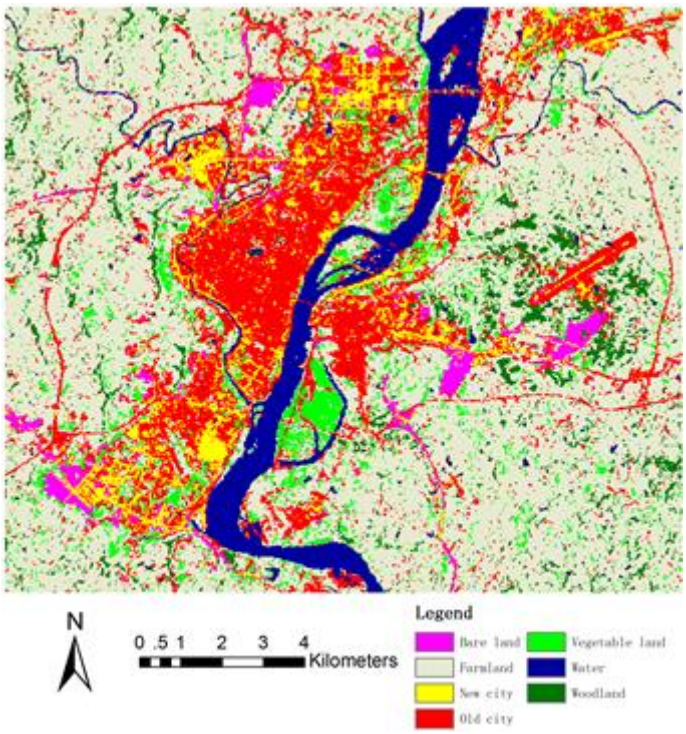

Figure 6. The Classification Using Spectrum Information and Normalized Difference Indexes

Total 3182 test samples were carefully selected from the original image, and the number of each category' test samples is about 500. The test samples were respectively input into the two trained network. The error matrix of classification is respectively shown as table 1 and table 2. Among them, table 1 is the result of using band 1-5 and 7 as the input of improved RBF network, table 2 is the result of using band 1-5, 7, SAVI, MNDWI and NDBI as the input of improved RBF network.

Table 1. The Classification Confusion Matrix Using Spectrum Information (Overall Accuracy = 89.97%, Kappa Coefficient = 0.88)

Classification	Reference data						
	bare land	new city	old city	water	woodland	farmland	vegetable land
bare land	473	26	19	1	2	2	1
new city	22	468	23	1	2	4	2
old city	15	35	520	3	9	9	7
water	1	1	1	527	2	1	2
woodland	4	2	9	8	465	16	20
farmland	2	3	6	5	21	481	31
vegetable land	2	1	2	2	19	35	465
Producer's accuracy (%)	91.14	87.31	89.66	96.34	89.42	87.77	88.07

From the table 1, we can find that the Overall accuracy is 89.97%, Kappa Coefficient is 0.88 when using the TM band 1~5 and 7 as the input of the improved RBF network. Because the spectral characteristics of bare land, new city and the old city are close, there are some misclassifications between each other, the Overall accuracy is between 87.31% and 91.14%. Because woodland, cultivated land and vegetable land are belong to

vegetation cover ground object, their spectral characteristics are similar, and the classification results may have some misclassification, the Overall classification accuracy are between 87.77% and 89.42%. But the classification accuracy of water is the highest, which is up to 96.34%.

Table 2. The Classification Confusion Matrix Using Spectrum Information and Normalized Indexes (Overall Accuracy = 95.02%, Kappa Coefficient = 0.94)

Classification	Reference data						
	bare land	new city	old city	water	woodland	farmland	vegetable land
bare land	495	15	11	0	1	1	0
new city	12	496	13	0	0	2	1
old city	8	19	541	1	4	5	4
water	1	0	2	542	0	0	0
woodland	2	2	7	1	502	6	7
farmland	1	3	4	3	8	519	21
vegetable land	0	1	2	0	5	15	495
Producer's accuracy (%)	95.38	92.54	93.28	99.09	96.54	94.71	93.75

From the table 2, we can find that the Overall accuracy is increased from 89.97% to 95.02% when SAVI, MNDVI and NDBI were added as the input of the improved RBF network, and the Overall accuracy was raised 5.05 percentage points. And the classification accuracy of each ground object is increased. Among them, the classification accuracy of the bare land, new city, old city, which are easy to mistake, is increased by 4.24%, 5.22%, 3.62%, respectively. The classification accuracy of the woodland, cultivated land and vegetable land, whose spectral characteristics are similar, is increased by 7.12%, 6.93% and 5.68%, respectively. The classification accuracy of water body is still the highest, is up to 99.09%. In conclusion, the classification accuracy can be improved at a certain extent when normalized spectral indexes with physical significance are added as the input of RBF network. The normalized difference indexes can extend the spectral difference especially for the ground objects whose original band information is close.

In order to further analyze the remote sensing classification model based on improved RBF neural network, the classification accuracy of improved RBF network, the maximum likelihood method and BP neural network are compared, the results as shown in table 3.

Table 3. The Classification Accuracies of Different Classification Algorithms

Classification Algorithms	Used Features	Overall Accuracy (%)	Kappa Coefficient
MLC	b1~b5,b7	85.68	0.84
BP	b1~b5,b7	88.54	0.87
Improved RBF	b1~b5,b7	89.97	0.88
MLC	b1~b5,b7,MNDWI,SAVI,NDBI	90.12	0.89
BP	b1~b5,b7,MNDWI,SAVI,NDBI	93.63	0.92
Improved RBF	b1~b5,b7,MNDWI,SAVI,NDBI	95.02	0.94

From the table 3, we can find that the classification accuracy of improved RBF neural network is close to or higher than BP neural network, and is significantly higher than maximum likelihood whether using band 1-5 and 7 as the input feature or using band 1-5, 7, SAVI, MNDWI and NDBI as the input feature. So, the remote sensing classification

model, based on the improved RBF network learning algorithm and adding normalized difference indexes as the input of network, can obtain higher classification accuracy for urban area with complex ground objects and discrete spatial distribution.

4. Conclusions

According to the complexity of the urban object types and the difficulty to distinguish the spectral characteristics of object types, the normalized difference indexes as MNDWI, ASVI and NDBI, were extracted from spectral information to be used as key auxiliary information of urban land use classification. The maximum minimum distance method was used to initialize the RBF center to solve the problem that the clustering algorithms can easily be trapped into local minima because of the random initialization of the RBF centers. And the balance factor was introduced into Gauss function to solve the problem that the value of output layer is very discrete because Gauss kernel function is used in the RBF neural network. On this basis, the urban remote sensing classification model was built based on improved RBF neural network and the normalized indexes. The experiments with the TM images showed that the built urban remote sensing classification model in this paper can effectively reduce the classification error of the bare land and the built-up and of the forest land and the cultivated land. The overall classification accuracy based on spectral information and indexes can be up to 95.02%, which was 5.05 percentage points than the overall accuracy based on only the spectral information. Experiments also showed that RBF neural network has a larger advantage than the traditional maximum likelihood method in fusing parameters as vegetation index, construction index, and so on.

It is difficult to determine the number of the intermediate RBF nodes, and which is the difficulty of RBF structure design. In this paper, the number of the intermediate RBF nodes was determined by many experiments. Further work is to establish some adaptive methods to automatically determine the number of intermediate nodes of RBF, so as to build the reasonable RBF network structure.

Acknowledgments

This work was supported by the Scientific and Technological Research Program of Chongqing Municipal Education Commission (KJ120517, KJ1402801) , the postdoctoral science funded project of Chongqing (XM20120019), the Program for National Natural Science Foundation of China (41201332) and the science and technology nova special of the Guangzhou Pearl River (2013J2200073). The authors also wish to thank the Institute of Remote Sensing and Digital Earth Chinese Academic of Sciences for the availability of the satellite data.

References

[1] P. Edoardo, M. Farid and T. Devis, “SVM active learning approach for image classification using spatial information [J]”, IEEE Transactions on Geoscience and Remote Sensing, vol. 52, no. 4, **(2014),** pp. 2217-2223.

[2] R. Zhang, D. Sun and S. Li, “A stepwise cloud shadow detection approach combining geometry determination and SVM classification for MODIS data [J]”, International Journal of Remote Sensing, vol. 34, no. 1, **(2013),** pp. 211-226.

[3] B. Andreas, W. Uwe and H. Stefan, “Classification in high dimensional feature spaces assessment using SVM, IVM and RVM with focus on simulated EnMAP data [J]”, IEEE Journal of Selected Topics in Applied Earth Observations and Remote Sensing, vol. 5, no. 2, **(2012),** pp. 436-443.

[4] P. Du, K. Tan and X. Xing, “Wavelet SVM in Reproducing Kernel Hilbert Space for hyper spectral remote sensing image classification [J]”, Optics Communications, vol. 283, no. 24, **(2010),** pp. 4978-4984.

[5] K. Abbas, E. Hamid and F. A. Farshid, “Design and implementation of an expert interpreter system for intelligent acquisition of spatial data from aerial or remotely sensed images [J]”, Journal of the International Measurement Confederation, vol. 47, no. 1, **(2014),** pp. 676-685.

[6] W. Elizabeth, N. David and R. Atiqur, "Expert system classification of urban land use/cover for Delhi, India [J]", International Journal of Remote Sensing, vol. 29, no. 15, **(2008),** pp. 4405-4427.
[7] S. J. Chen, Y. H. Hu and D. J. Sun, "Classification of hyper spectral remote sensing image based on nonlinear kernel mapping and artificial immune network [J]", Journal of Infrared and Millimeter Waves, vol. 33, no. 3, **(2014),** pp. 289-296.
[8] X. J. Bo, S. L. Sheng and Z. D. Fu, "Remote sensing image classification based on a modified self-organizing neural network with a priori knowledge [J]", Sensors and Transducers, vol. 153, no. 6, **(2013**), pp. 29-36.
[9] H. Min, X. Zhu and Y. Wei, "Remote sensing image classification based on neural network ensemble algorithm [J]", Neurocomputing, vol. 78, no. 1, **(2012),** pp. 133-138.
[10] L. Kai, L. Xu and F. Zhong Ke, "Application of SOFM neural network in classification of remote sensing images [J]", Journal of Beijing Forestry University, vol. 30(SUPPL 1), **(2008),** pp. 73-77.
[11] C. Solares and A. M. Sanz, "Bayesian network classifiers. An application to remote sensing image classification [J]", WSEAS Transactions on Systems, vol. 4, no. 4, **(2005),** pp. 343-348.
[12] K. Tan and P.-J. Du, "Hyperspectral remote sensing image classification based on radical basis function neural network [J]", Spectroscopy and Spectral Analysis, vol. 28, no. 9, **(2013),** 2009-2013.
[13] L. J. Cheng, M. D. Ping and S. Z. Feng, "Elliptical basis function network for classification of remote-sensing images [J]", Journal of Data Acquisition and Processing, vol. 20, no. 1, **(2005),** pp. 8-12.
[14] B. Lorenzo and P. D. Fernandez, "Technique for the selection of kernel-function parameters in RBF neural networks for classification of remote-sensing images [J]", IEEE Transactions on Geoscience and Remote Sensing, vol. 37, no. 2, **(1999),** pp. 1179-1184.
[15] G. M. Foody, "Supervised image classification by MLP and RBF neural networks with and without an exhaustively defined set of classes [J]", International Journal of Remote Sensing, vol. 2, no. 15, **(2004),** pp. 3091-3104.
[16] L. H. Wan, S. C. Zhang and W.-Y. Liu, "A RBF classification method of remote sensing image based on genetic algorithm [J]", Journal of Harbin Institute of Technology, vol. 13, no. 6, **(2006),** pp. 711-714.
[17] L. Li and D. Li, "Applied PSO-RBF to aerial and satellite remote sensing image texture classification [J]", Geomatics and Information Science of Wuhan University, vol. 34, no. 9, **(2009),** pp. 1051-1054.
[18] Y. Zhong, L. Zhang and W. Gong, "Unsupervised remote sensing image classification using an artificial immune network [J]", International Journal of Remote Sensing, vol. 32, no. 19, **(2011),** pp. 5461-5483.
[19] S. H. Liu and S. Ning, "Design of classifier for remote sensing image based on RBF networks [J]", Journal of Geomatics, vol. 31, no. 2, **(2006),** pp. 10-13.
[20] M. A. Shaban and O. Dikshit, "Improvement of classification in urban areas by the use of textural features: The case study of Lucknow city, Uttar Pradesh [J]", International Journal of Remote Sensing, vol. 22, no. 4, **(2001),** pp. 565-593.
[21] D. Rob, "Texture analysis and classification of ERS SAR images for map updating of urban areas in the Netherlands [J]", IEEE Transactions on Geoscience and Remote Sensing, vol. 41, no. 9, **(2003),** pp.1950-1958.
[22] W. Su, J. Li and Y. Chen, "Textural and local spatial statistics for the object-oriented classification of urban areas using high resolution imagery [J]", International Journal of Remote Sensing, vol. 29, no. 11, **(2008),** pp. 3105-3117.
[23] M. A. Aguilar, M. M. Saldaña, F. J. Aguilar, "GeoEye-1 and WorldView-2 pan-sharpened imagery for object-based classification in urban environments [J]", International Journal of Remote Sensing, vol. 34, no. 7, **(2013),** pp. 2583-2606.
[24] D. Pinho, C. M. Duque, F. L. M. Garcia, "Land-cover classification of an intra-urban environment using high-resolution images and object-based image analysis [J]", International Journal of Remote Sensing, vol. 33, no. 19, **(2012),** pp. 5973-5995.
[25] T. S. Purevdorj, R. Tateishi and T. Ishiyama, "Relationships between percent vegetation cover and vegetation indices [J]", International Journal of Remote Sensing, vol. 19, **(1998),** pp. 3519-3535.
[26] A R. Huete, "A Soil-Adjusted Vegetation Index (SAVI) [J]", Remote Sensing of Enviroment, vol. 25, **(1988),** pp. 195-309.
[27] Y. Zha, J. Gao and S. Ni, "Use of normalized difference built-up index in automatically mapping urban areas from TM imagery [J]", International Journal of Remote Sensing, vol. 24, **(2005),** pp. 583-594.
[28] S K. McFeeters , "The use of normalized difference water index (NDWI) in the delineation of open water features [J]", International Journal of Remote Sensing, vol. 17, no. 7, **(1996),** pp. 1425-1432.
[29] XUHQ, "A study on information extraction of water body with the modified normalized difference water index (MNDWI) [J]", Journal of Remote Sensing, vol. 9, no. 5, **(2005),** pp. 589-595.
[30] X. Luo, Q. Liu and Q. Liu, "Research on Remote Sensing Classification Based on Improved Kohonen Neural Network [J]", 2nd International Conference on Computer Engineering and Technology, vol. 4, **(2010),** pp. 545-547.
[31] X. Luo and X. Liu, "The Application of Self Organizing Neural Networks to Remote Sensing Image Classification [J]", Remote Sensing for Land & Resources, vol. 4, **(2004),** pp. 14-17.

Authors

Xiaobo Luo, he is an associate professor of Chongqing University of Post and Telecommunications, China. His current research interests mainly include thermal infrared remote sensing and its application in urban thermal environment and ecological environment monitoring and evaluating.

Wenya Zhao, she is an associate professor of Chongqing Aerospace Vocational and Technological College, China. Her current research interests mainly include image processing and urban environment.

Shiqiang Wei, he is a professor of Southwest China University, China. His current research interests mainly include urban environment and ecological environment monitoring and evaluation.

Qinghua Fu, he is an associate researcher of Pearl River Hydraulic Research Institute , Pearl River Water Resources Commission, China. His current research interests mainly include ecological environment monitoring and evaluating.